Effects of inorganic electrolyte anions on enrichment of Cu(II) ions with aminated Fe₃O₄/graphene oxide: Cu(II) speciation prediction and surface charge measurement

CrossMark

Xin-jiang Hu [a,b], Yun-guo Liu [a,b,*], Guang-ming Zeng [a,b], Hui Wang [a,b], Shao-hong You [c], Xi Hu [a,b], Xiao-fei Tan [a,b], An-wei Chen [d], Fang-ying Guo [a,b]

[a] College of Environmental Science and Engineering, Hunan University, Changsha 410082, PR China
[b] Key Laboratory of Environmental Biology and Pollution Control (Hunan University), Ministry of Education, Changsha 410082, PR China
[c] College of Environmental Science and Engineering, Guilin University of Technology, Guilin 541004, PR China
[d] College of Resources and Environment, Hunan Agricultural University, Changsha 410128, PR China

HIGHLIGHTS

- Divalent anions had bigger effects on Cu(II) adsorption than monovalent anions.
- Both monovalent and divalent anions could alter the zeta potential of AMGO.
- Divalent inorganic electrolyte anions could significantly affect Cu(II) species.
- HPO_4^{2-} had the biggest effect on Cu(II) removal in the multi-ion system.
- Interactions of $Cl^- \times SO_4^{2-}$ and $Cl^- \times SO_4^{2-}$ had big effects on Cu(II) removal.

ARTICLE INFO

ABSTRACT

The present work evaluated the effects of six inorganic electrolyte anions on Cu(II) removal using aminated Fe₃O₄/graphene oxide (AMGO) in single- and multi-ion systems. A 2^{6-2} fractional factorial design (FFD) was employed for assessing the effects of multiple anions on the adsorption process. The results indicated that the Cu(II) adsorption was strongly dependent on pH and could be significantly affected by inorganic electrolyte anions due to the changes in Cu(II) speciation and surface charge of AMGO. In the single-ion systems, the presence of monovalent anions (Cl^-, ClO_4^-, and NO_3^-) slightly increased the Cu(II) adsorption onto AMGO at low pH, while the Cu(II) adsorption was largely enhanced by the presence of SO_4^{2-}, CO_3^{2-}, and HPO_4^{2-}. Based on the estimates of major effects and interactions from FFD, the factorial effects of the six selected species on Cu(II) adsorption in multi-ion system were in the following sequence: $HPO_4^{2-} > CO_3^{2-} > Cl^- > SO_4^{2-} > NO_3^- = ClO_4^-$, and the combined factors of AD ($Cl^- \times SO_4^{2-}$) and EF ($Cl^- \times SO_4^{2-}$) had significant effects on Cu(II) removal.

1. Introduction

Adsorption is a popular and economical method for treating metal pollutions in natural water and wastewater (Babel and Kurniawan, 2003; Lam et al., 2008). Many studies have shown that heavy metals could be efficiently adsorbed by a wide variety of adsorbents (Babel and Kurniawan, 2003; Lam et al., 2008; Bui and Choi, 2010; Liu et al., 2011; Hu et al., 2013). Graphene oxide (GO) is an ideal material for removing heavy metals from aqueous solution due to its exceptional physicochemical properties. In recent years, magnetic graphene oxide composites (MGO) have been synthesized and shown some good properties for water treatment due to that the integration of magnetic properties into GO combines the advantages of adsorption with the merit of easy separation (Liu et al., 2011; Li et al., 2012; Hu et al., 2013). Diethylenetriamine (DETA), an organic compound, contains three amino groups that are known to form stable complexes with various metals. Therefore, grafting DETA onto MGO surface may increase the adsorption capacity of MGO for metal ions.

* Corresponding author at: College of Environmental Science and Engineering, Hunan University, Changsha 410082, PR China. Tel.: +86 731 88649208; fax: +86 731 88822829.
E-mail address: hnuese@126.com (Y.-g. Liu).

It is well known that adsorption behavior of heavy metals in water is controlled by adsorbent properties, heavy metal species, and water characteristics (Bui and Choi, 2010). The composition of heavy metal wastewaters from different industries varies widely. Generally, industrial wastewaters contain not only heavy metal ions but also high concentrations of organic and inorganic substances. Inorganic electrolyte anions, such as chloride (Cl^-), nitrate (NO_3^-), sulfate (SO_4^{2-}), phosphate ($H_2PO_4^-/HPO_4^{2-}$), and bicarbonate/carbonate (HCO_3^-/CO_3^{2-}), are commonly present in natural water and wastewater systems (Zhu et al., 2007), and these anions can affect metal cations adsorption directly or indirectly (Doula and Ioannou, 2003). Thus, investigation of the influence of inorganic electrolyte anions on heavy metals adsorption is essential to evaluate the adsorption capacity of an adsorbent and apply the laboratory results to practical projects. Although previous studies have given some insights into the influences of anions on adsorption of heavy metals, more research is still needed to better understand the influence mechanism.

Inorganic electrolyte anions play important roles in the speciation of metal ions due to that the metal ions often exist in bulk aqueous phase as complexes with ligands (Doula and Ioannou, 2003). The metal–ligand complexes may be adsorbed only weakly or not at all by the adsorbent, thereby inhibiting the metal ions removal. If the metal–ligand complexes are precipitates or can be strongly adsorbed by the adsorbent, the adsorption of metal ions may be improved by the presence of the inorganic electrolyte anions (Doula and Ioannou, 2003). Therefore, reliable methods for predicting metal speciation are critically needed as the first step in determining the influence mechanism of anions on adsorption of heavy metals. Besides, the inorganic electrolyte anions may interact with the adsorbent surface, thereby altering the surface electrical properties. Zeta potential is widely used to quantify the magnitude of the electronic charge on adsorbent surfaces. Thus, the observable changes in zeta potential due to the effects of inorganic electrolyte anions can provide valuable insight into the potential changes in metal ions removal during water treatment processes (Pommerenk and Schafran, 2005).

The main objectives of this study were to: (1) prepare AMGO by grafting DETA onto MGO surface and apply it as an adsorbent for decontamination of Cu(II) from aqueous solution; (2) evaluate the influences of inorganic electrolyte anions on the adsorption of Cu(II) onto AMGO; (3) discuss the influence mechanism by analyzing the speciation of metal ions and evaluating the effects of inorganic electrolyte anions on the zeta potential of the adsorbent; (4) determine the important factors and the extent of each individual ion effect on the Cu(II) removal using fractional factorial design (FFD).

2. Materials and methods

2.1. Synthesis of AMGO

Graphene oxide (GO) and magnetic graphene oxide (MGO) were prepared following the methods described in our previous papers (Hu et al., 2013, 2014a). The aminated Fe_3O_4/graphene oxide (AMGO) was prepared by grafting DETA onto the MGO surface (Ma et al., 2012). Briefly, 0.9 mL ammonia solution was added into 100 mL MGO suspension (3 mg mL^{-1}) and the mixture was stirred for 5 min at room temperature. Then 3.6 mL diethylenetriamine was added, and the suspension was stirred for 10 min at room temperature, and then stirred at 95 °C for another 6 h. The obtained AMGO was rinsed with ethanol and Milli-Q water for several times and stored at room temperature.

2.2. Effects of single anions on adsorption process

All adsorption experiments were performed according to the batch method in conical flasks on an orbital shaker with a shaking speed of 150 rpm. The stock solution of Cu(II) and the stock suspension of AMGO were added to achieve the desired concentrations of the different components. To investigate the adsorptive efficiency of AMGO for Cu(II) in the presence of various inorganic electrolyte anions, NaCl, $NaClO_4$, $NaNO_3$, Na_2SO_4, Na_2CO_3 and Na_2HPO_4 were added into the conical flasks, respectively. After mixed for 24 h, the mixture was separated by a magnetic process using a permanent magnet. The Cu(II) concentration in the supernatant was analyzed using flame atomic absorption spectrometry (PerkinElmer AA700, USA). All batch experiments were conducted in triplicates and the data are expressed as mean ± standard deviation. The adsorption capacity (q_e) of Cu(II) adsorbed on AMGO was calculated from the difference between the initial concentration (C_0) and the equilibrium concentration (C_e) (Gong et al., 2011).

2.3. Zeta potential determination

The samples were prepared by ultrasonification of 9.6 mg AMGO with 500 mL of solution in the absence and presence of 10 mM inorganic electrolyte anions (Cl^-, ClO_4^-, NO_3^-, SO_4^{2-}, CO_3^{2-}, and HPO_4^{2-}) and the solution pH was adjusted to different values (2–11). Then, the zeta potentials were measured using a Zetasizer Nano SZ (ZEN3690, Malvern, UK).

2.4. Speciation modeling methods

In order to analyze the effects of inorganic electrolyte anions on copper speciation in aqueous solution under different pH conditions, Visual MINTEQ (ver. 3.1) was used for the chemical speciation calculations. The parameters were set as follows: pH was fixed at different values; temperature was 30 °C; ionic strength was to be calculated depending on components added; different concentrations of $Cu(NO_3)_2$ and inorganic electrolyte anions were added as components (Hu et al., 2014b).

2.5. Fractional factorial design

In order to evaluate the statistical significance of the effects of the six different inorganic electrolyte anions and their interactions on Cu(II) removal, the 2^{6-2} FFD with resolution IV was developed. The confounded (aliased) factors and the interactions for this 2^{6-2} FFD are explained in detail in literature (Tanboonchuy et al., 2012). The design matrix of the 2^{6-2} FFD and the levels of each stated anion are given in Table 1. Statistical analysis of the fractional factorial design was performed using the software Design-Expert 8.0.6 (Stat-Ease Inc., Minneapolis, MN, USA).

3. Results and discussion

3.1. Effects of monovalent anions

The effects of monovalent anions (Cl^-, ClO_4^-, and NO_3^-) on Cu(II) adsorption as a function of pH values were examined and the results are demonstrated in Fig. 1a–c. The adsorption of Cu(II) onto AMGO increased with the increase of pH values from 2 to 11 in the absence and presence of monovalent inorganic electrolyte anions. As well known, solution pH is one of the most important variables affecting the adsorption process because the pH affects not only the adsorbent surface charge and ionization, but also the speciation of adsorbate (Hameed and El-Khaiary, 2008). In order to quantify the magnitude of electronic charge on adsorbent surfaces, the zeta

Table 1
Experimental design matrix of the 2^{6-2} FFD with resolution IV[a]: $C_{0(Cu)}$ = 10 mg L^{-1}, m/V = 96 mg L^{-1}, T = 30 °C, t = 24 h, pH = 5.5.

Run no.	A Cl$^-$	B ClO$_4^-$	C NO$_3^-$	D SO$_4^{2-}$	E = A × B × C CO$_3^{2-}$	F = B × C × D HPO$_4^{2-}$	q_e (mg g^{-1})
1	−	−	+	+	+	−	67.08 ± 2.04
2	−	−	−	−	−	−	56.37 ± 0.75
3	−	+	+	+	−	+	69.20 ± 2.09
4	−	−	−	+	−	+	76.41 ± 1.53
5	+	+	−	+	−	−	55.71 ± 1.88
6	+	+	+	+	+	+	79.58 ± 0.45
7	+	−	−	−	+	−	78.44 ± 1.58
8	+	−	−	+	+	+	80.71 ± 3.23
9	+	+	−	−	−	+	85.23 ± 2.23
10	−	+	+	−	−	−	50.26 ± 2.97
11	+	−	+	−	−	+	78.73 ± 3.70
12	+	−	+	+	−	−	59.65 ± 1.47
13	+	+	+	−	+	−	77.92 ± 0.73
14	−	+	−	+	+	−	67.34 ± 3.25
15	−	+	−	−	+	+	80.57 ± 3.45
16	−	−	+	−	+	+	83.37 ± 2.45
17	0	0	0	0	0	0	30.94 ± 1.16

[a] The minus (−) and plus (+) signs indicate the low and high levels of the factors, respectively. The test levels (low, high) in mM of codes A through F are as follows: (1, 100) for A, B, C, D, and E; (1, 50) for F.

potentials of AMGO under various pH (2–11) in the absence of background electrolyte ions were determined and the results are showed in the inset of Fig. 1a. The pH$_{pzc}$ value (point of zero charge) for AMGO was 5.94. At pH < pH$_{pzc}$, the surfaces of AMGO were positively charged, while the AMGO surfaces were negatively charged when pH > pH$_{pzc}$. Distribution of Cu(II) species as a function of solution pH in the system without background electrolyte ions was obtained using the program visual MINTEQ and the results (Fig. 2a) demonstrated that the Cu(II) presented mainly in the form of Cu^{2+}, Cu(OH)$^+$, Cu(OH)$_2$, Cu$_2$(OH)$_2^{2+}$, Cu$_3$(OH)$_4^{2+}$ and Cu(OH)$_3^-$ at various pH values. At pH < 5.94, the uptake of Cu(II) was small, which was probably due to that the positive Cu^{2+} ions were difficult to adsorb on the positively charged surfaces of AMGO because of the electrostatic repulsion (Zhao et al., 2011). The precipitation curve of Cu(II) calculated from the precipitation constant of Cu(OH)$_2$(s) (K_{sp} = 2.2 × 10^{-20}) at the concentration of 10 mg L^{-1} is presented in Fig. 2b. It is clear that Cu(II) started to form precipitation at pH 6.07. Therefore, at pH > 5.94, the high adsorption capacity was achieved mainly due to the cooperating role of precipitation of Cu(OH)$_2$ and adsorption of Cu^{2+}, Cu(OH)$^+$, Cu$_2$(OH)$_2^{2+}$, and Cu$_3$(OH)$_4^{2+}$ onto AMGO (Li et al., 2012).
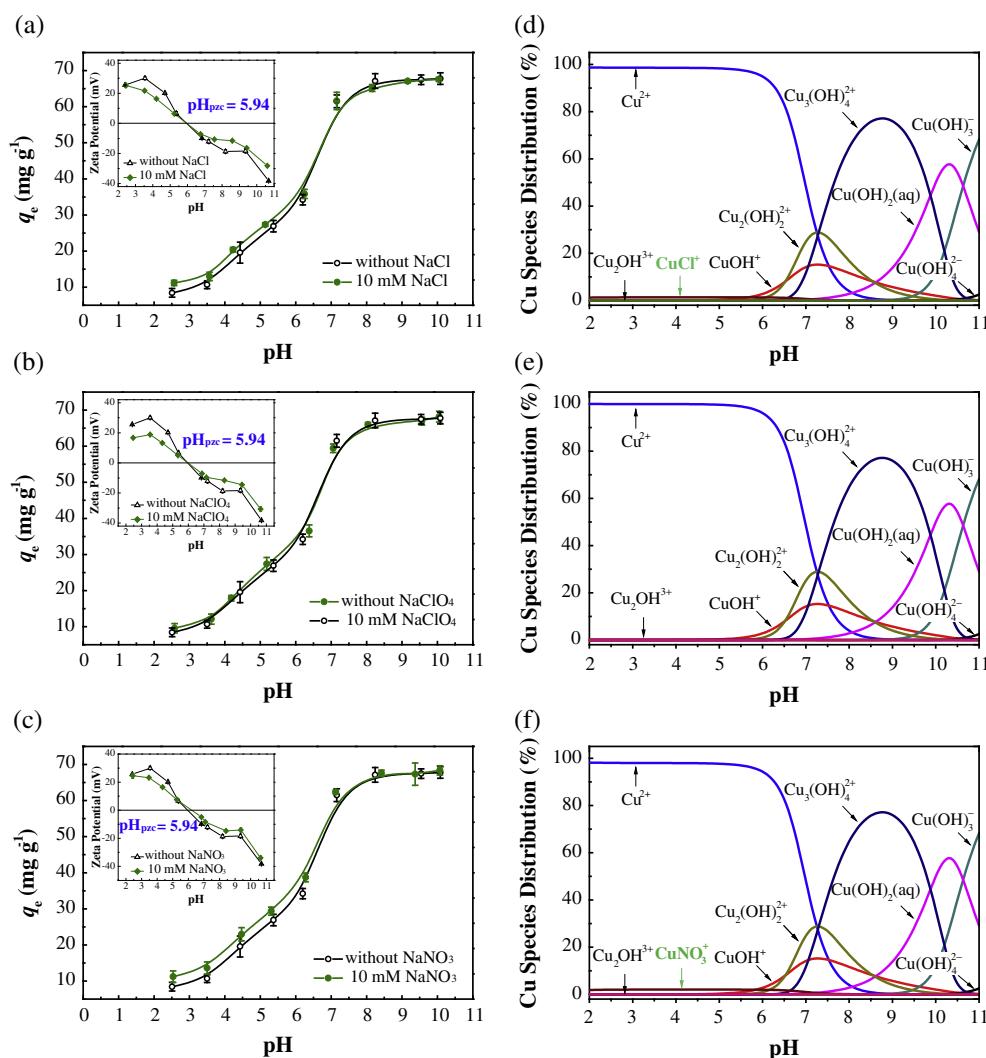
Fig. 1. Effects of (a) Cl$^-$, (b) ClO$_4^-$, and (c) NO$_3^-$ in solution (concentration = 10 mM) on Cu(II) adsorption onto AMGO at different pH (the insets show the effects of Cl$^-$, ClO$_4^-$, NO$_3^-$ on the measured zeta potential, respectively): $C_{0(Cu)}$ = 10 mg L^{-1}, m/V = 96 mg L^{-1}, T = 30 °C, t = 24 h; distribution of Cu(II) species in solution with addition of 10 mM, (d) Cl$^-$, (e) ClO$_4^-$, and (f) NO$_3^-$ as a function of pH computed by the program visual MINTEQ: $C_{0(Cu)}$ = 10 mg L^{-1}, T = 30 °C.

From Fig. 1a–c, the presence of Cl^-, ClO_4^-, and NO_3^- slightly increased the Cu(II) adsorption at low pH, whereas no significant changes in Cu(II) adsorption to the AMGO composites were observed at high pH. It is well known that the copper speciation in equilibrium solution is influenced by accompanying anions (Yu et al., 2005). Distributions of Cu(II) in solution with addition of 10 mM NaCl, $NaClO_4$, and $NaNO_3$, as a function of solution pH were obtained by using the program Visual MINTEQ and the results are showed in Fig. 1d–f. We can see that the distributions of Cu(II) species in 10 mM NaCl (Fig. 1d), $NaClO_4$ (Fig. 1e), and $NaNO_3$ (Fig. 1f) solutions were very similar to the distribution of Cu(II) species in solution without background electrolyte ions (Fig. 2a). Therefore, the effects of these monovalent anions on Cu(II) species were negligible. The enhancement of Cu(II) adsorption by NaCl, $NaClO_4$, and $NaNO_3$ may be mainly ascribed to the interaction of the monovalent inorganic electrolyte anions with the adsorbent surface. Zeta potential can be used to indicate the potential difference between the dispersion medium and the stationary layer of fluid attached to the dispersed particles (Ding et al., 2013). The changes in zeta potential as a function of solution pH in the absence and presence of 10 mM Cl^-, ClO_4^-, and NO_3^- are presented in the insets of Fig. 1a–c, respectively. Addition of NaCl, $NaClO_4$, and $NaNO_3$ decreased the zeta potentials at pH < pH_{pzc}, but increased the zeta potentials at pH > pH_{pzc}. Coordination might be the main mechanism for Cu(II) adsorption onto AMGO at pH < 5.94. The decrease in zeta potential of adsorbent reduced the electrostatic repulsion forces between the positive Cu^{2+} and the positively charged surfaces of AMGO, therefore the Cu^{2+} ions were more accessible to the adsorption sites and then these ions could be captured by forming coordinate covalent bonds. No drastic difference of Cu(II) adsorption to the AMGO composite in NaCl, $NaClO_4$, and $NaNO_3$ solutions was observed at high pH, which was most probably due to the surface precipitates at high pH values (Liu et al., 2011).

3.2. Effects of divalent anions

Fig. 3a–c shows the effects of divalent anions on the adsorption of Cu(II) onto AMGO as a function of pH in 10 mM Na_2SO_4, Na_2CO_3, and Na_2HPO_4 solutions, respectively. As can be observed, the presence of SO_4^{2-}, CO_3^{2-}, and HPO_4^{2-} largely improved the Cu(II) adsorption, and different background anions had different influences on the Cu(II) removal. These phenomena could be explained by the formation of neutral complexes ($CuSO_4$, $CuCO_3$, and $CuHPO_4$) and the interaction of SO_4^{2-}, CO_3^{2-}, and HPO_4^{2-} with adsorbent surface. As seen from Fig. 3d, the main Cu(II) species in the solution with presence of 10 mM SO_4^{2-} were Cu^{2+} and $CuSO_4$ at pH < 7. The neutral $CuSO_4$ complex could be more easily adsorbed by the positively charged AMGO than the Cu^{2+}, thereby resulting in the

increase of Cu(II) removal. The effect of SO_4^{2-} on Cu(II) adsorption was also related to the change of zeta potential caused by anion adsorption (Yu et al., 2005). From the inset of Fig. 3a, when 10 mM Na_2SO_4 was presented in the system, the zeta potentials of AMGO decreased obviously at pH < 6.8, but increased slightly at pH > 6.8, and the pH_{pzc} value for AMGO in this solution was 4.56. The decrease of electrostatic potential at the adsorption plane favored the specific adsorption of Cu(II) occurring on AMGO because of the decrease in electrostatic repulsion of positively charged AMGO surfaces to Cu^{2+} (Jiang et al., 2010). There are other mechanisms for explaining the enhancement of Cu^{2+} adsorption by SO_4^{2-}. Lam et al. (2008) indicated that the Cu^{2+} adsorption required at least two sites and could not adsorb on the isolated sites. The SO_4^{2-} stabilized the Cu^{2+} adsorption on the individual amino sites, that is, the SO_4^{2-} could act as one of the adsorption sites, therefore improving the adsorption capacity for Cu(II) ions (Lam et al., 2008). Besides, the amino groups on AMGO surface might interact with the hydroxyl group by hydrogen bond. The SO_4^{2-} in solution could liberate these amino groups for more Cu^{2+} adsorption and further participate by forming a stable complex with the adsorbed Cu^{2+} (Lam et al., 2008).

The effect of CO_3^{2-} on the adsorption of Cu(II) onto AMGO composite is shown in Fig. 3b. As can be seen, the presence of CO_3^{2-} in solution noticeably increased the Cu(II) removal. From Fig. 3e, the Cu(II) species in solution with presence of 10 mM CO_3^{2-} were quite different from those in the solution without CO_3^{2-} (Fig. 2a). The predominant Cu(II) species was Cu^{2+} at pH < 6. From the inset of Fig. 3b, the presence of CO_3^{2-} decreased the zeta potentials of AMGO, which could be due to the interaction of the CO_3^{2-} with the double layer of AMGO, thereby resulting in the increase of Cu(II) adsorption at pH < 6. In the pH range of 6–9, the main Cu(II) species was $CuCO_3$. And some of $CuCO_3$ could be hydrolyzed to form copper hydroxide, which combined with the residual $CuCO_3$ to form copper carbonate basic. The copper carbonate basic could precipitate from solution and then be adsorbed by the AMGO. At pH > 9, the carbonate ions could coadsorb with Cu^{2+} to form stable complexes with sufficient strength to travel with the AMGO particles, which resulted in the increase of Cu(II) adsorption.

Fig. 3c shows that the presence of Na_2HPO_4 improved the Cu(II) removal. The inset of Fig. 3c indicated that the zeta potential of AMGO in the system with Na_2HPO_4 was lower in the whole pH range than that in the system without Na_2HPO_4. The observed decrease in the zeta potential values might be due to that HPO_4^{2-} could occupy the inner-sphere adsorption sites on the AMGO surface and therefore lowered the surface electrostatic potential near the solid surface (Li et al., 2006). From Fig. 3f, in the system with presence of 10 mM Na_2HPO_4, Cu(II) species could be present mainly in the forms of Cu^{2+}, $CuHPO_4(aq)$, $Cu(OH)^+$, $Cu(OH)_2$, $Cu_2(OH)_2^{2+}$, $Cu_3(OH)_4^{2+}$ and $Cu(OH)_3^-$ at various pH values. There are four possible

Fig. 2. (a) Distribution of Cu(II) species in solution without adding inorganic electrolyte anions as a function of pH computed by the program visual MINTEQ: $C_{0(Cu)}$ = 10 mg L^{-1}, T = 30 °C; (b) the precipitation curve of Cu(II) at the concentration of 10 mg L^{-1} (K_{sp} = 2.2 × 10^{-20}).
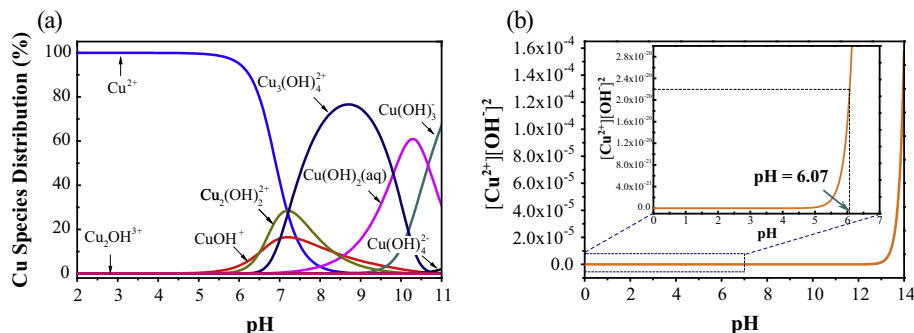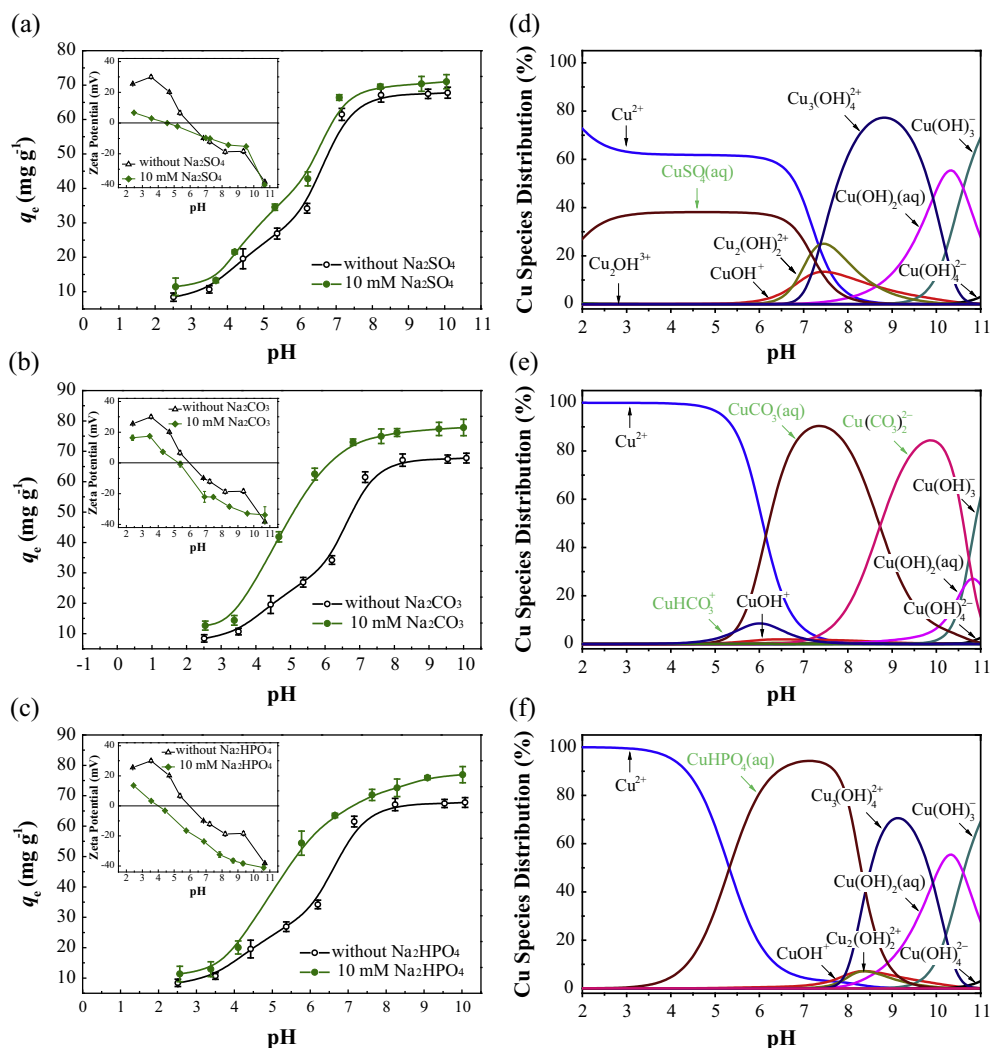
Fig. 3. Effects of (a) SO_4^{2-}, (b) CO_3^{2-}, and (c) HPO_4^{2-} in solution (concentration = 10 mM) on Cu(II) adsorption onto AMGO at different pH (the insets show the effects of SO_4^{2-}, CO_3^{2-}, and HPO_4^{2-} on the measured zeta potential, respectively): $C_{0(Cu)}$ = 10 mg L^{-1}, m/V = 96 mg L^{-1}, T = 30 °C, t = 24 h; distribution of Cu(II) species in solution with addition of 10 mM, (d) SO_4^{2-}, (e) CO_3^{2-}, and (f) HPO_4^{2-} as a function of pH computed by the program visual MINTEQ: $C_{0(Cu)}$ = 10 mg L^{-1}, T = 30 °C.

reasons for the increase of Cu(II) removal in the presence of Na$_2$HPO$_4$: (1) the decrease in zeta potential of AMGO surface due to the adsorption of negative HPO_4^{2-} made the positively charged Cu(II) ions much easier to be captured by adsorption sites (Sheng et al., 2014); (2) the Cu(II) ions could be captured by the adsorbed HPO_4^{2-} and then formed a ternary cation–anion–surface complex (Collins et al., 1999); (3) the HPO_4^{2-} could enhance the Cu(II) adsorption by stabilizing the Cu^{2+} adsorption on the unfavorable sites and by anchoring CuHPO$_4$ complex on the isolated amino sites (Lam et al., 2008); (4) the metal–ligand complex could precipitate from solution, thereby resulting in the increase of the Cu(II) removal.

3.3. FFD for assessing effect of multiple anions

The FFD, an efficient tool for evaluating a large number of variables with a reasonable number of experimental runs, can help us elucidate the effects of single and multiple factors on the problem of concern (Chang et al., 2011; Tanboonchuy et al., 2012). It has advantages over more standard methods in those instances where the important variables are not known or are many, and it also allows codependencies among experimental variables to be tested statistically (Aziz et al., 2011). In order to find the relative importance of individual background anions on Cu(II) adsorption and

identify important interactions between pairs of anions (Steinle et al., 2000), FFD experiments were conducted in aqueous solution in the presence of six selected species with concentrations of different levels, and the results are demonstrated in Table 1. As shown in Table 1, the adsorption capacity of AMGO for Cu(II) ions in the system without background anions (Run 17) was 30.94 mg g^{-1}. However, the adsorption capacities in the system with presence of different concentrations of the six background anions were found to range from 50.26 to 85.23 mg g^{-1}, indicating that the Cu(II) adsorption was largely enhanced by the presence of the six background anions. The relatively higher and lower Cu(II) removal were found in Run 9 and 10, respectively.

The estimates of 2^{6-2} FFD with resolution IV are showed in Fig. 4. The main effect for each of variables is the difference between the average response of high level variables (+) and the average response of low level variables (−) in the design matrix of Table 1 (Hsu et al., 2008; Tanboonchuy et al., 2012). From Fig. 4, the positive estimates of main effects of A(Cl$^-$), E(CO$_3^{2-}$), F(HPO$_4^{2-}$) were 5.67, 10.43, and 15.13, respectively, indicating that adsorption capacity of AMGO for Cu(II) ions increased when the concentration of these background anions increased from low level to high level. For example, when the NaCl and Na$_2$CO$_3$ concentrations in solutions increased from 1 to 100 mM, the average

Fig. 4. Identification of main effective factors and interaction factors on Cu(II) removal by AMGO.

adsorption capacities deceased from 74.50 to 68.83 mg g^{-1} for NaCl and from 76.88 to 66.45 mg g^{-1} for Na$_2$CO$_3$. Besides, increasing Na$_2$HPO$_4$ concentration from 1 to 50 mM resulted in the decrease of Cu(II) removal by 15.13 mg g^{-1}, which was equal to 79.23 mg g^{-1} (the average response of high level) minus 64.10 mg g^{-1} (the average response of high level). According to Fig. 4, we can also find that the negative estimates of main effects of B(ClO$_4^-$), C(NO$_3^-$), and D(SO$_4^{2-}$) were −1.87, −1.87, and −4.40, respectively. This is to say that the Cu(II) removal decreased with increasing the concentrations of these background anions from 1 to 100 mM. In summary, in the system with presence of multiple background anions, the factorial effects of the six selected species on the adsorption of Cu(II) ions by AMGO were found to be in the following order: HPO$_4^{2-}$ > CO$_3^{2-}$ > Cl$^-$ > SO$_4^{2-}$ > NO$_3^-$ = ClO$_4^-$.

The two-factor interaction effect can be determined as half the difference between the main effects of one factor at the two levels of a second factor (Mason et al., 1989; Secula et al., 2013). The combined effect of the two factors is not the sum of their separate contributions, but it indicates antagonism or synergism between the two factors (Hsu et al., 2008; Tanboonchuy et al., 2012). According to FFD generation structure, the AD interaction (Cl$^-$ × SO$_4^{2-}$) is confounded with the EF interaction (CO$_3^{2-}$ × HPO$_4^{2-}$) (Secula et al., 2013). From Fig. 4, the combined factors of AD and EF were found to have more significant effect than the other interaction factors on Cu(II) adsorption.

An interaction plot is a graphical tool which plots the mean response of two factors at all possible combinations of their settings (Antony, 2003; Pokhrel and Viraraghavan, 2008). Non-parallel lines indicate that there is interaction between the two factors. If the lines are parallel, the two factors have no interactions (Antony, 2003). The interaction effects of the six background anions for Cu(II) removal are presented in Fig. 5. As seen from Fig. 5, all lines in the 30 cells were non-parallel, indicating that any two background anions in the aqueous solution had interactions. The angles between two lines in cell AD (or DA) and cell EF (or FE) were bigger than others, which implied that there were rather strong two-way interactions between the main effects of Cl$^-$ and SO$_4^{2-}$ and between the main effects of CO$_3^{2-}$ and HPO$_4^{2-}$.

Fig. 5. Interaction effects plot for Cu removal: (A) Cl$^-$, (B) ClO$_4^-$, (C) NO$_3^-$, (D) SO$_4^{2-}$, (E) CO$_3^{2-}$, and (F) HPO$_4^{2-}$.

This finding is in consistence with the result in Fig. 4. These inter-action effects cannot be detected in univariate statistic techniques (Montgomery et al., 2006). From Fig. 5, we can also single out important factors for interaction within each cell (Tanboonchuy et al., 2012). In Column A, all adsorption capacities of AMGO for Cu(II) ions in cells except the cell AD (high D) increased with increasing NaCl concentration from low level (1 mM) to high level (100 mM). For the cells (except the cell AD) in Columns B, C and D, the Cu(II) removal decreased slightly as the concentrations of $NaClO_4$, $NaNO_3$, and Na_2SO_4 increased form 1 mM to 100 mM, respectively. However, for the cells in Columns E and F, significant slope of each line within each cell was observed, which indicated that increasing factors E and F from low to high level resulted in the significant enhancement of Cu(II) uptake.

4. Conclusions

The AMGO can be used as an adsorbent for Cu(II) removal from aqueous solution, and the adsorption capacity increases with increasing the pH from 2 to 11. The adsorption characteristics of AMGO for Cu(II) ions can be affected by the presence of various inorganic electrolyte anions. The removal of Cu(II) ions is slightly improved by the presence of 10 mM Cl^-, ClO_4^-, and NO_3^- at low pH due to the reduction of electrostatic repulsion forces between the positive Cu^{2+} and the positively charged AMGO surface, while no significant changes in Cu(II) adsorption are observed at high pH. The presence of SO_4^{2-}, CO_3^{2-}, and HPO_4^{2-} in the system can significantly enhance Cu(II) adsorption, and these divalent anions have bigger influences on the adsorption process than the monovalent anions at various pH values, which may be due to that both monovalent and divalent anions can alter the zeta potential of AMGO, but only the divalent anions can significantly affect the Cu(II) species. The estimates of main effects of the six selected species and their interactions in the multiple species system attained from FFD reveal that increasing the concentrations of A(Cl^-), E(CO_3^{2-}), F(HPO_4^{2-}) and/or decreasing the concentrations of B(ClO_4^-), C(NO_3^-), D(SO_4^{2-}) from low to high level can enhance the Cu(II) adsorption onto AMGO. In the multiple species system, the effects of the six selected species on Cu(II) removal are in the order of: $HPO_4^{2-} > CO_3^{2-} > Cl^- > SO_4^{2-} > NO_3^- = ClO_4^-$. Besides, any two background anions in the multi-ion system have interactions, and the combined factors of AD ($Cl^- \times SO_4^{2-}$) and EF ($CO_3^{2-} \times HPO_4^{2-}$) have more significant effects than the other interaction factors on Cu(II) adsorption.

Acknowledgements

References

Antony, J., 2003. Design of Experiments for Engineers and Scientists. Butterworth-Heinemann, Burlington.

Aziz, B., Zhao, G., Hedin, N., 2011. Carbon dioxide sorbents with propylamine groups-silica functionalized with a fractional factorial design approach. Langmuir 27, 3822–3834.

Babel, S., Kurniawan, T.A., 2003. Low-cost adsorbents for heavy metals uptake from contaminated water: a review. J. Hazard. Mater. 97, 219–243.

Bui, T.X., Choi, H., 2010. Influence of ionic strength, anions, cations, and natural organic matter on the adsorption of pharmaceuticals to silica. Chemosphere 80, 681–686.

Chang, S.H., Teng, T.T., Ismail, N., 2011. Screening of factors influencing Cu(II) extraction by soybean oil-based organic solvents using fractional factorial design. J. Environ. Manage. 92, 2580–2585.

Collins, C.R., Ragnarsdottir, K.V., Sherman, D.M., 1999. Effect of inorganic and organic ligands on the mechanism of cadmium sorption to goethite. Geochim. Cosmochim. Ac 63, 2989–3002.

Ding, D., Lei, Z., Yang, Y., Feng, C., Zhang, Z., 2013. Nickel oxide grafted andic soil for efficient cesium removal from aqueous solution: adsorption behavior and mechanisms. Acs Appl. Mater. Interfaces 5, 10151–10158.

Doula, M.K., Ioannou, A., 2003. The effect of electrolyte anion on Cu adsorption-desorption by clinoptilolite. Micropor. Mesopor. Mater. 58, 115–130.

Gong, J., Liu, T., Wang, X., Hu, X., Zhang, L., 2011. Efficient removal of heavy metal ions from aqueous systems with the assembly of anisotropic layered double hydroxide nanocrystals@carbon nanosphere. Environ. Sci. Technol. 45, 6181–6187.

Hameed, B.H., El-Khaiary, M.I., 2008. Malachite green adsorption by rattan sawdust: isotherm, kinetic and mechanism modeling. J. Hazard. Mater. 159, 574–579.

Hsu, J.C., Lin, C.J., Liao, C.H., Chen, S.T., 2008. Evaluation of the multiple-ion competition in the adsorption of As(V) onto reclaimed iron-oxide coated sands by fractional factorial design. Chemosphere 72, 1049–1055.

Hu, X.-J., Liu, Y.-G., Wang, H., Chen, A.-W., Zeng, G.-M., Liu, S.-M., Guo, Y.-M., Hu, X., Li, T.-T., Wang, Y.-Q., Zhou, L., Liu, S.-H., 2013. Removal of Cu(II) ions from aqueous solution using sulfonated magnetic graphene oxide composite. Sep. Purif. Technol. 108, 189–195.

Hu, X.-J., Liu, Y.-G., Zeng, G.-M., Wang, H., Hu, X., Chen, A.-W., Wang, Y.-Q., Guo, Y.-M., Li, T.-T., Zhou, L., Liu, S.-H., Zeng, X.-X., 2014a. Effect of aniline on cadmium adsorption by sulfanilic acid-grafted magnetic graphene oxide sheets. J. Colloid Interface Sci. 426, 213–220.

Hu, X.-J., Liu, Y.-G., Zeng, G.-M., You, S.-H., Wang, H., Hu, X., Guo, Y.-M., Tan, X.-F., Guo, F.-Y., 2014b. Effects of background electrolytes and ionic strength on enrichment of Cd(II) ions with magnetic graphene oxide–supported sulfanilic acid. J. Colloid Interface Sci. 435, 138–144.

Jiang, J., Xu, R.K., Li, S.Z., 2010. Effect of ionic strength and mechanism of Cu(II) adsorption by Goethite and γ-Al₂O₃. J. Chem. Eng. Data 55, 5547–5552.

Lam, K.F., Chen, X., McKay, G., Yeung, K.L., 2008. Anion effect on Cu²⁺ adsorption on NH₂-MCM-41. Ind. Eng. Chem. Res. 47, 9376–9383.

Li, J., Zhang, S.W., Chen, C.L., Zhao, G.X., Yang, X., Li, J.X., Wang, X.K., 2012. Removal of Cu(II) and fulvic acid by graphene oxide nanosheets decorated with Fe₃O₄ nanoparticles. Acs Appl. Mater. Interfaces 4, 4991–5000.

Li, W., Zhang, S., Jiang, W., Shan, X.Q., 2006. Effect of phosphate on the adsorption of Cu and Cd on natural hematite. Chemosphere 63, 1235–1241.

Liu, M.C., Chen, C.L., Hu, J., Wu, X.L., Wang, X.K., 2011. Synthesis of magnetite/graphene oxide composite and application for cobalt(II) removal. J. Phys. Chem. C 115, 25234–25240.

Ma, H.L., Zhang, Y.W., Hu, Q.H., Yan, D., Yu, Z.Z., Zhai, M.L., 2012. Chemical reduction and removal of Cr(VI) from acidic aqueous solution by ethylenediamine-reduced graphene oxide. J. Mater. Chem. 22, 5914–5916.

Mason, R.L., Gunst, R.F., Hess, J.L., 1989. Statistical Design and Analysis of Experiments with Applications to Engineering and Science. John Wiley & Sons Inc, New York.

Montgomery, D.C., Runger, G.C., Hubele, N.F., 2006. Engineering Statistics. John Wiley & Sons Inc., New York.

Pokhrel, D., Viraraghavan, T., 2008. Organic arsenic removal from an aqueous solution by iron oxide-coated fungal biomass: an analysis of factors influencing adsorption. Chem. Eng. J. 140, 165–172.

Pommerenk, P., Schafran, G.C., 2005. Adsorption of inorganic and organic ligands onto hydrous aluminum oxide: evaluation of surface charge and the impacts on particle and NOM removal during water treatment. Environ. Sci. Technol. 39, 6429–6434.

Secula, M., Cretescu, I., Cagnon, B., Manea, L., Stan, C., Breaban, I., 2013. Fractional factorial design study on the performance of gac-enhanced electrocoagulation process involved in color removal from dye solutions. Materials 6, 2723–2746.

Sheng, T., Baig, S.A., Hu, Y., Xue, X., Xu, X., 2014. Development, characterization and evaluation of iron-coated honeycomb briquette cinders for the removal of As(V) from aqueous solutions. Arabian J. Chem. 7, 27–36.

Steinle, P., Thalmann, P., Hohener, P., Hanselmann, K.W., Stucki, G., 2000. Effect of environmental factors on the degradation of 2,6-dichlorophenol in soil. Environ. Sci. Technol. 34, 771–775.

Tanboonchuy, V., Grisdanurak, N., Liao, C.H., 2012. Background species effect on aqueous arsenic removal by nano zero-valent iron using fractional factorial design. J. Hazard. Mater. 205–206, 40–46.

Yu, S., He, Z.L., Huang, C.Y., Chen, G.C., Calvert, D.V., 2005. Effects of anions on the capacity and affinity of copper adsorption in two variable charge soils. Biogeochemistry 75, 1–18.

Zhao, G.X., Li, J.X., Ren, X.M., Chen, C.L., Wang, X.K., 2011. Few-layered graphene oxide nanosheets as superior sorbents for heavy metal ion pollution management. Environ. Sci. Technol. 45, 10454–10462.

Zhu, X., Nanny, M.A., Butler, E.C., 2007. Effect of inorganic anions on the titanium dioxide-based photocatalytic oxidation of aqueous ammonia and nitrite. J. Photochem. Photobiol., A 185, 289–294.